Available online at www.sciencedirect.com

ScienceDirect

journal homepage: www.elsevier.com/locate/he

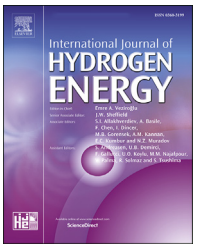

Modelling, simulation and control of a fuel cell-powered laptop computer voltage regulator module

Y. RavindranathTagore [a,*], K. Anuradha [b], Attuluri R. Vijay Babu [c], P. Manoj Kumar [d]

[a] Vignan's Lara Institute of Technology and Science, Guntur-522213, India
[b] VNR VJ Institute of Engineering and Technology, Hyderabad-500090, India
[c] Vignan's Foundation for Science, Technology & Research, Guntur-522213, India
[d] PSG Institute of Technology and Applied Research, Coimbatore-641062, India

ARTICLE INFO

Article history:
Received 13 July 2018
Received in revised form
17 November 2018
Accepted 20 February 2019
Available online xxx

Keywords:
Air-breathing fuel cell
Power conditioning unit
Quadratic buck converter
Average current mode control

ABSTRACT

An air-breathing fuel cell was investigated as an alternate power source for a laptop computer application. An empirical model was developed to include the phenomena of activation and ohmic polarisation as well as mass transport effects in order to simulate the behaviour of an air-breathing fuel cell. The model was used as the input source for a quadratic buck converter, which is used to power the central processing unit (CPU) core at 1 V. To achieve tight voltage regulation and good dynamic performance, the quadratic buck converter was implemented with average current mode control. The quadratic buck converter hardware setup has been developed with a fabricated fuel cell module in order to validate the model of the air-breathing fuel cell as well as the voltage regulator module.

© 2019 Hydrogen Energy Publications LLC. Published by Elsevier Ltd. All rights reserved.

Introduction

A fuel cell is an electrochemical device that converts the chemical energy of a fuel and an oxidant (pure oxygen or air) directly into electricity, eliminating the intermediate step of classical, chemical combustion used in the normal process of heat extraction from fuel [1,2]. Since it is a direct single step energy conversion device, it contributes to high electrical efficiency. Moreover, the fuel cell uses pure hydrogen for the electrochemical reaction, giving water, heat and electricity as products, and so is a clean source of energy. These characteristic features [3] of the fuel cell, i.e., high efficiency, zero/low pollutant emission and fuel flexibility, make it an extremely desirable option for future power generation. Proton exchange membrane fuel cells (PEMFCs), alternatively referred to as polymer electrolyte membrane fuel cells, fall under the category of low-temperature fuel cells. During the reaction, the hydrogen at the anode gets oxidized to protons through the release of electrons. The protons move from the anode to the cathode through the proton conducting electrolyte, while the electrons move through the external circuit to reach the cathode. At the cathode, oxygen combines with the protons emanating from the membrane as well as the electrons from the external load circuit to produce water and heat according to reactions (1)–(3).

* *Corresponding author.*
E-mail address: yrtagore@gmail.com (Y. RavindranathTagore).
https://doi.org/10.1016/j.ijhydene.2019.02.141
0360-3199/© 2019 Hydrogen Energy Publications LLC. Published by Elsevier Ltd. All rights reserved.

Please cite this article as: RavindranathTagore Y et al., Modelling, simulation and control of a fuel cell-powered laptop computer voltage regulator module, International Journal of Hydrogen Energy, https://doi.org/10.1016/j.ijhydene.2019.02.141

Nomenclature

V	Voltage, V
A_C	Active area of cell, cm^2
ΔV	Overpotential, V
V_{Cr}	Voltage loss due to crossover, V
i	Current density, mA/cm^2
i_{Cr}	Crossover current, mA/cm^2
p	Partial pressure of hydrogen, bar
P	Pressure of hydrogen, bar
P_{Sat}	Saturation pressure of water, bar
r	Ohmic resistance, Ω-cm^2
L	Thickness of membrane, cm
T	Temperature, K
K	Proportionality constant
Z	Zero of a transfer function
P	Pole of a transfer function
D	Duty cycle
i_L	Limiting current density, mA/cm^2
i_o	Exchange current density, mA/cm^2

Greek letters

α	Charge transfer coefficient
λ	Water drag coefficient
σ	Conductivity of membrane, S/cm
ρ	Specific resistance, Ω-cm

$$\text{At the anode}: 2H_2 \rightarrow 4H^+ + 4e^- \quad (1)$$

$$\text{At the cathode}: O_2 + 4H^+ + 4e^- \rightarrow 2H_2O \quad (2)$$

$$\text{Overall reaction}: 2H_2 + O_2 \rightarrow 2H_2O + \text{Electricity} + \text{Heat} \quad (3)$$

Fuel cells that take up oxygen by passive means from ambient air for the reaction at the cathode are known as air-breathing fuel cells (ABFC) [4–6]. In ABFCs, oxygen is supplied to the cathode through free convection air flow and hydrogen is supplied to the anode from compressed gas cylinders. Free convection oxygen delivery at the cathodes of ABFCs eliminates the need for an auxiliary fan or compressor (air circulating device) as in forced convection fuel cells. The considerable reduction in weight and volume of the overall system makes it more viable for commercialization, especially in portable electronic devices like laptops. Also, to mitigate the inflammable nature of hydrogen, air is preferred over oxygen. Under normal operation, a single ABFC typically produces 0.5 V–0.7 V. Several ABFCs are connected in series to form an ABFC stack.

Besides the ABFC, other significant system components are the power conditioning unit (PCU) and their controllers. Switched mode power supplies (SMPSs) play a vital role for processing power in modern gadgets because of their high efficiency and compactness. They call for wide conversion ratios, for example 1 V, 1.5 V, 3.3 V and 12 V power supplies. Existing buck converters are unable to support such conversions as their switches demand minimum ON time [7]. Moreover, a cascade connection achieves wider conversion ratios, although it may compromise the overall efficiency owing to switching losses in the metal oxide semiconductor field effect transistors (MOSFETs). This paper proposes the quadratic buck converter (QBC), an advanced dc-dc converter as a viable ABFC stack PCU [8]. The converter circuit when applied to laptop computer voltage regulator module reduces the dc voltage of 19 V obtained from the fuel stack to 1 V. The paper will shed light on the behaviour of the ABFC by comparing the characteristics obtained through PSIM simulation [9] with the experimental results of a commercial fuel cell module.

ABFC power system model

The power system model implemented here consists of the following sections:

- PSIM model of an ABFC stack.
- PSIM model of QBC with average current mode (ACM) control technique.

The proposed ABFC Power system schematic is shown in Fig. 1. The modelling of each section is explained in the succeeding sections.

Development, experimental investigation and validation of the ABFC model

Development of ABFC stack model

To simplify the analysis, the following assumptions are made.

a) All gases obey the ideal gas law.
b) Hydrogen gas supplied to the anode is pure.
c) The hydrogen and oxygen temperatures are equal to the cell temperature.
d) Constant pressure in the gas flow channels.
e) Liquid water is the only reaction product.

The standard potential of a hydrogen/oxygen fuel cell at STP (25 °C and 1 atm) is 1.229 V when liquid water is the product. However, due to irreversible losses, there is a decrease from its equilibrium potential. The three types of irreversible losses present in ABFCs are activation, concentration and ohmic losses. The output voltage of the single cell ABFC [10–12] is represented by Eqs. 4–10.

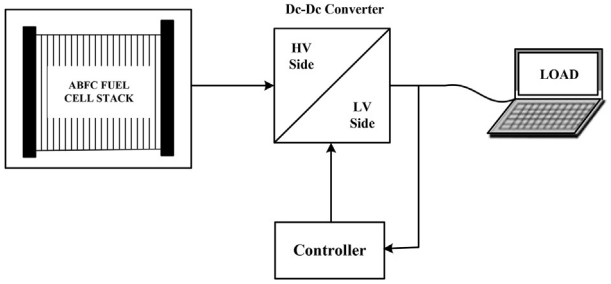

Fig. 1 – Proposed ABFC stack power conditioning unit.

Please cite this article as: RavindranathTagore Y et al., Modelling, simulation and control of a fuel cell-powered laptop computer voltage regulator module, International Journal of Hydrogen Energy, https://doi.org/10.1016/j.ijhydene.2019.02.141

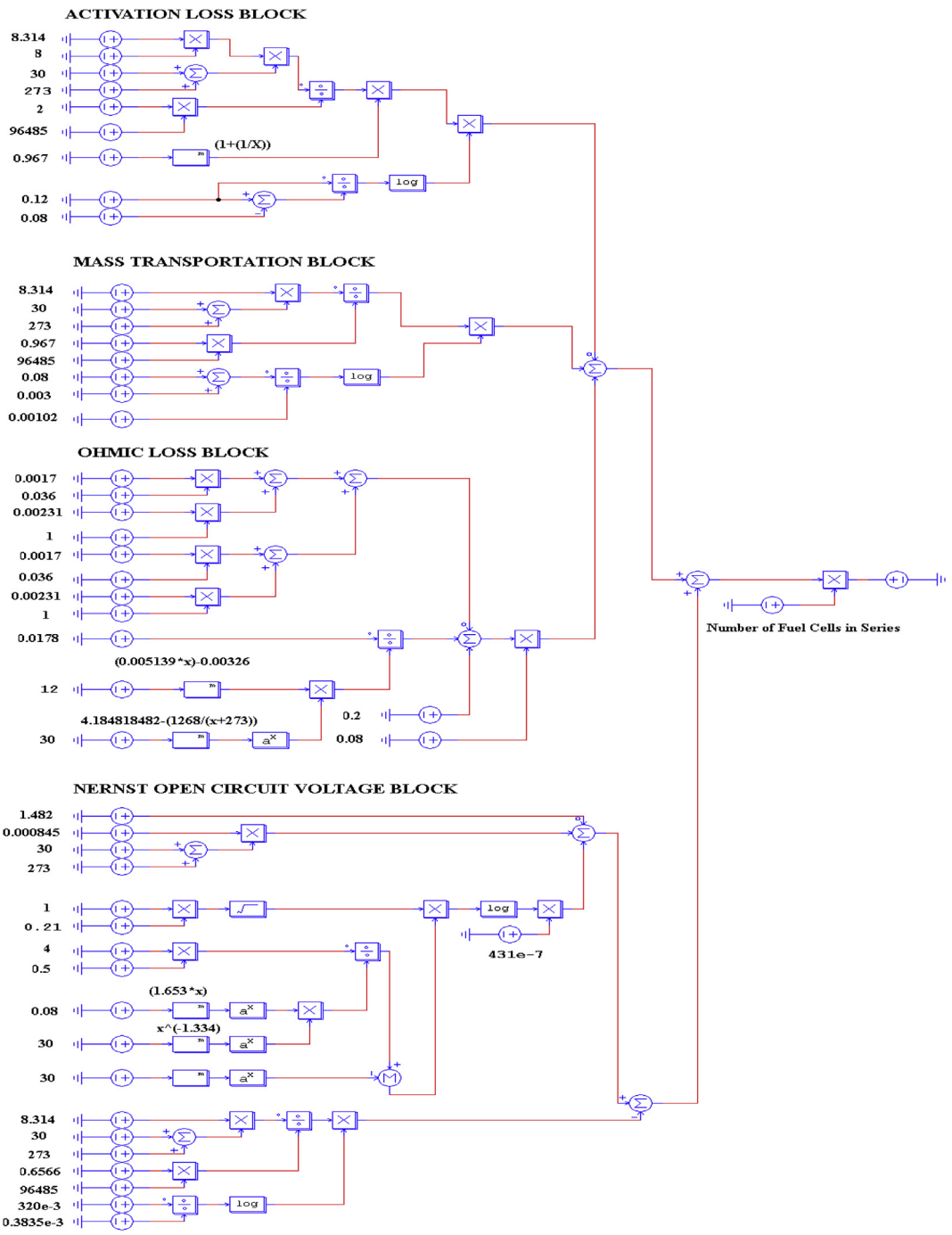

Fig. 2 – Scheme of the model developed in PSIM in order to simulate single cell behaviour under steady state conditions.

$$V_{Fuelcell} = V_{Opencircuit} - \Delta V_{Activation} - \Delta V_{Ohmic} - \Delta V_{Concentration} \quad (4)$$

$$V_{Opencircuit} = V_{Nernst} - V_{Crossover} \quad (5)$$

$$V_{Nernst} = 1.482 - 0.000845*T + 0.0000431*T*\ln\left(\rho_{H_2} * \rho_{O_2}^{0.5}\right) \quad (6)$$

$$V_{Crossover} = \frac{RT}{\alpha F}\ln\left(\frac{i_{Crossover}}{i_0}\right) \quad (7)$$

Table 1 – Simulation parameters of the ABFC.

Parameter	Value
Specific resistance of GDL	0.0017 Ω-cm
Thickness of GDL	0.036 cm
Specific resistance of graphite	0.00231 Ω-cm
Thickness of graphite flow channel	0.1 cm
Thickness of membrane	0.0178 cm
Water drag coefficient	12
Crossover current	3 mA/cm^2
Contact resistance	30 Ω-cm^2

Please cite this article as: RavindranathTagore Y et al., Modelling, simulation and control of a fuel cell-powered laptop computer voltage regulator module, International Journal of Hydrogen Energy, https://doi.org/10.1016/j.ijhydene.2019.02.141

Fig. 3 – Fuel cell test setup.

$$\rho_{H_2} = \frac{0.5P_{H_2}}{\exp\left(\frac{1.653*i}{T_{ADP}^{1.334}}\right)} - P_{Sat} \quad (8)$$

$$\rho_{O_2} = \frac{P_{O_2}}{\exp\left(\frac{4.192*i}{T_{GDP}^{1.334}}\right)} - P_{Sat} \quad (9)$$

$$P_{Sat} = 10^{\left(-2.1794+0.02953*T-9.1837*10^{-5}*T^2+1.4454*10^{-7}*T^2\right)} \quad (10)$$

It is necessary to overcome the limitation of the activation energy barrier to initiate the reaction at the electrodes. The activation loss represents the energy spent by the ABFC in crossing the barrier and is modelled according to Eq. (11).

Table 2 – Electro chemical parameters of the ABFC.

Temperature	Charge transfer coefficient (α)	Exchange current density (i_O)
30° C	0.967	1.02 mA/cm^2
40° C	0.725	1.662 mA/cm^2

$$\Delta V_{Activation} = \frac{RT}{\alpha F}\ln\left(\frac{i}{i_0}\right) \quad (11)$$

Internal losses in an ABFC occur due to the diffusion of hydrogen molecules from the anode to the cathode and the

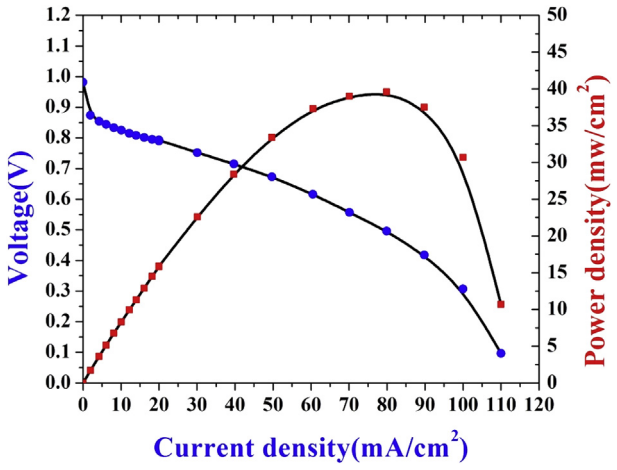

Fig. 4 – Polarisation characteristic of the single ABFC.

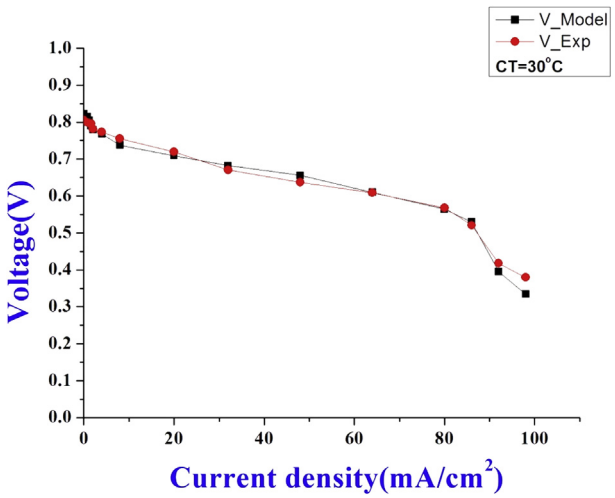

Fig. 5 – Validation of the ABFC at 30 °C.

Please cite this article as: RavindranathTagore Y et al., Modelling, simulation and control of a fuel cell-powered laptop computer voltage regulator module, International Journal of Hydrogen Energy, https://doi.org/10.1016/j.ijhydene.2019.02.141

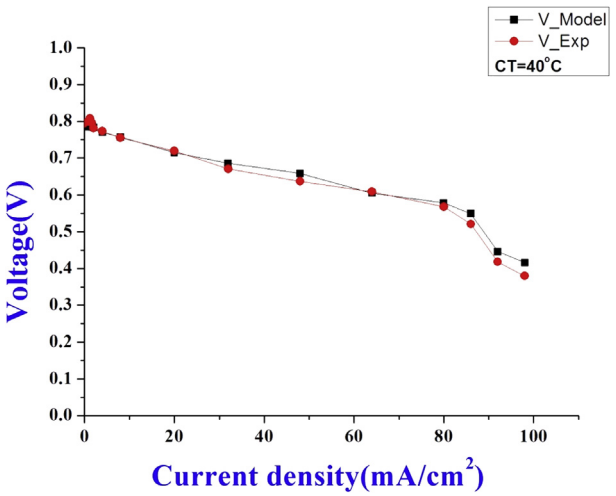

Fig. 6 – Validation of the ABFC at 40 °C.

movement of stray electrons through the membrane. These losses, although insignificant, can impair the cell potential considerably, especially when operating at very low current densities. To simulate this phenomenon, the term i_{loss} is incorporated into the current 'i' in Eq. (12) with a fixed value of 3 mA/cm^2 [12]. So, in a fuel cell the activation losses are:

$$\Delta V_{Activation} = \frac{RT}{\alpha F}\ln\left(\frac{i + i_{cr}}{i_0}\right) \quad (12)$$

The ohmic loss and resistance offered by an ABFC are represented by Eq. (13) and Eq. (14). Electrical and ionic resistances are modelled according to Eqs. 15–18 and the contact resistance is assigned a fixed value of 30 Ω-cm^2 [12].

$$\Delta V_{Ohmic} = i^* r_{Ohmic} \quad (13)$$

$$r_{Ohmic} = r_{Anode} + r_{Cathode} + r_{Ionic} + r_{Contact} \quad (14)$$

$$r_{Anode} = \frac{\rho_{GDL^*L_{GDL}}}{A_C} + \frac{\rho_{Graphite^*L_{Graphite}}}{A_C} \quad (15)$$

$$r_{Cathode} = \frac{\rho_{GDL^*L}}{A_C} + \frac{\rho_{Graphite^*L}}{A_C} \quad (16)$$

$$r_{Ionic} = \frac{L_{Membrane}}{\sigma A_C} \quad (17)$$

$$\sigma = (0.005169^*\lambda - 0.00326)^*\exp\left(1268\left(\frac{1}{303} - \frac{1}{T}\right)\right) \quad (18)$$

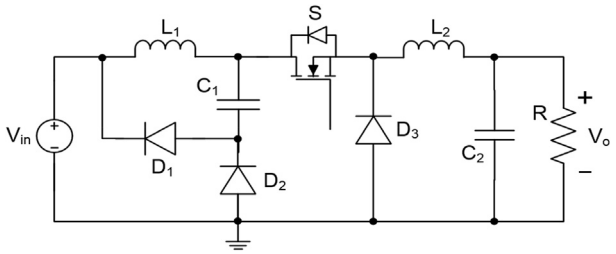

Fig. 7 – Schematic of quadratic buck converter.

Table 3 – Design specifications of the QBC.

Parameter	Value
Input voltage	19 V
Inductance (L_1)	1.84 μH
Inductance (L_2)	0.21 μH
Inductor resistance	0.95 mΩ
Capacitance (C_1)	22 μF
Capacitance (C_2)	1.64 mF
Capacitor (ESR)	1.67 mΩ
Switching frequency	300 KHz
Load resistance(min)	0.067Ω
Load resistance (max)	0.18 Ω
Output voltage	1 V

Concentration losses that occur due to the mass transfer of reactants at high current densities as well as the presence of concentration gradients can be expressed by Eq. (19).

$$\Delta V_{Concentration} = \frac{RT}{nF}\left(1 + \frac{1}{\alpha}\right)\ln\left(\frac{i_L}{i_L - i}\right) \quad (19)$$

The model built in PSIM is obtained from Eqs. 4–19 which are shown in Fig. 2. The ABFC model gives a steady-state polarisation curve as a function of anode dew point temperature, hydrogen pressure and cell temperature. The simulation parameters shown in Table 1 are taken from manufacturer data sheets and also the literature [12–14].

Experimental investigation

The fuel cell membrane electrode assembly (MEA) was fabricated with a 5-cm^2 active area, a Pt/C (40%) catalyst loading of 1 mg/cm^2 and 30% and 20% hydrophobisation on both the anode and cathode side. Nafion 117 was used as the electrolyte membrane. The 850e Compact Fuel Cell Test System was used for conducting the experiments on assembled single cell as shown in Fig. 3. The measured fuel cell characteristic at a cell temperature of 25 °C is shown in Fig. 4. The experimentally calculated values of charge transfer coefficient and exchange current density are tabulated in Table 2.

Validation of the ABFC model

The validation of the characteristics obtained from the PSIM model with those experimentally measured with the fuel cell at cell temperatures of 30 °C and 40 °C are depicted in Fig. 5

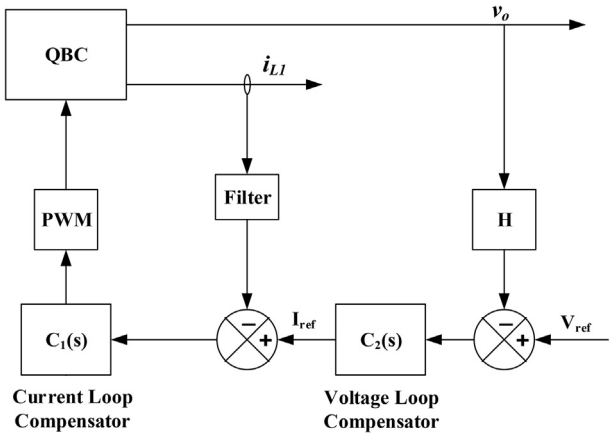

Fig. 8 – Block diagram of average current-mode controller.

Please cite this article as: RavindranathTagore Y et al., Modelling, simulation and control of a fuel cell-powered laptop computer voltage regulator module, International Journal of Hydrogen Energy, https://doi.org/10.1016/j.ijhydene.2019.02.141

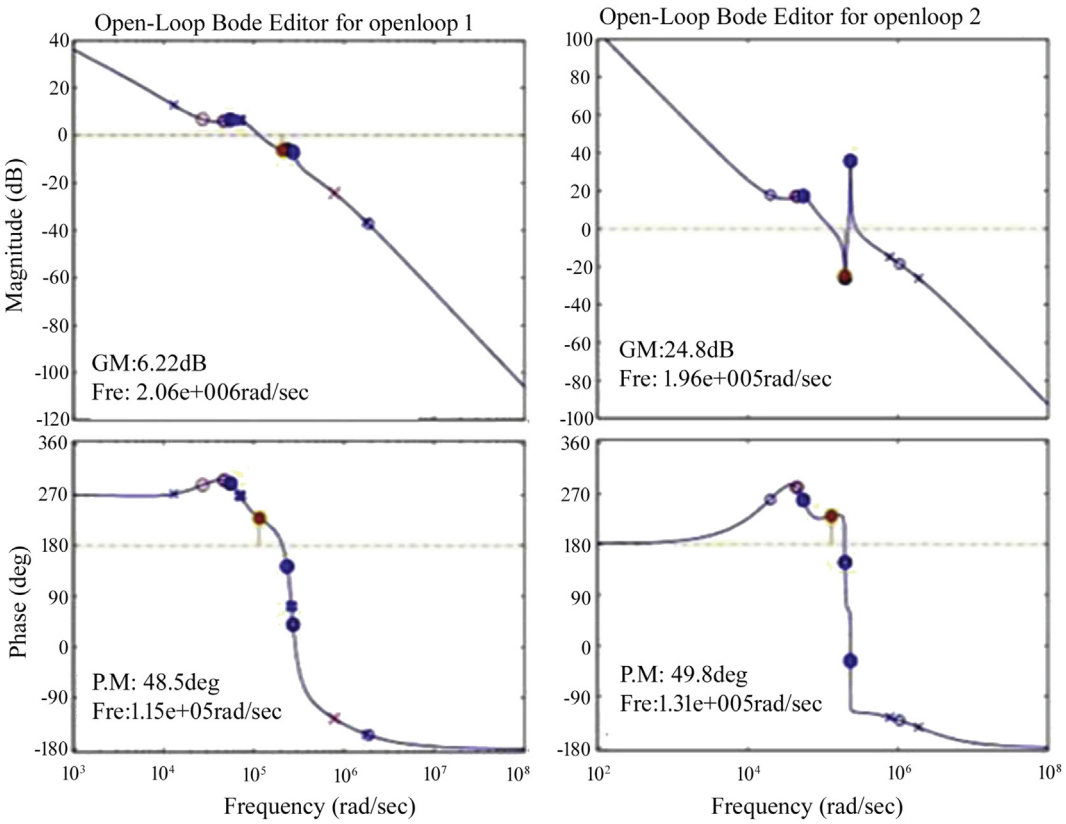

Fig. 9 – Bode plots for open loop gains of current and voltage loop.

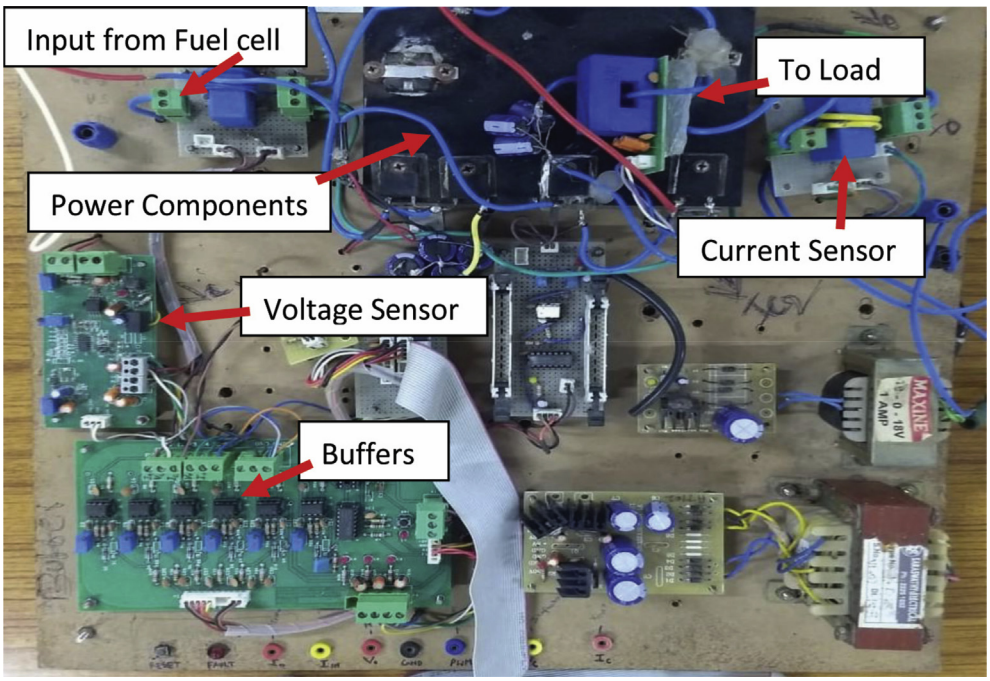

Fig. 10 – Hardware setup of quadratic buck converter.

Please cite this article as: RavindranathTagore Y et al., Modelling, simulation and control of a fuel cell-powered laptop computer voltage regulator module, International Journal of Hydrogen Energy, https://doi.org/10.1016/j.ijhydene.2019.02.141

and Fig. 6, respectively. There is good agreement in these results.

Design of the power conditioning unit and controller

Design of the quadratic buck converter

It is possible to achieve good dynamics with the incorporation of a power electronic processor, i.e., d.c.-to-d.c. converter. Also, when considered in view of the voltage deviation and settling time during load transients, better dynamic performance is possible. The QBC schematic is shown in Fig. 7. The QBC conversion ratio is modelled by Eq. (20). The values of the simulation parameters obtained from the design of the QBC are shown in Table 3.

$$M(D) = \frac{V_O}{V_{in}} = D^2 \tag{20}$$

Design of the average current mode controller

For continuous conduction mode based QBC, the control transfer functions exhibit right-half-plane (RHP) zeros [8]. These RHP zeros cause dramatic undershoots and longer settling time, particularly in voltage mode control based QBC. Nevertheless, ACM control [8] can overcome sluggish response as indicated in the block diagram of Fig. 8. ACM control has several dominant aspects over peak current mode control such as absence of noise and subharmonic oscillations. This paper presents ACM control based QBC for examining both the steady-state and dynamic behaviour.

Design of the current loop

The crossover frequency of the voltage loop is lower than the current loop. Also, the corner frequency of the low-pass filter is equal to the converter switching frequency. $C_1(s)$ is a lag compensator whose transfer function is represented by Eq. (21).

$$C_1(s) = \frac{K(s+Z_1)}{s} \tag{21}$$

Design of the voltage loop

$C_2(s)$ is a lag-lead compensator in the voltage loop whose transfer function is represented by Eq. (22).

$$C_2(s) = \frac{K(s+Z_1)(s+Z_2)}{s(s+P)} \tag{22}$$

The gain and phase margins for the stable current and voltage loops are 6.22 dB, 48.5° and 24.8 dB, 49.8°, respectively, as shown in Fig. 9. The experimental setup of the QBC is shown in Fig. 10.

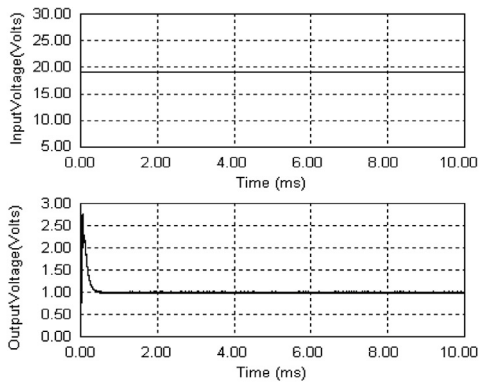

(a) Simulation results

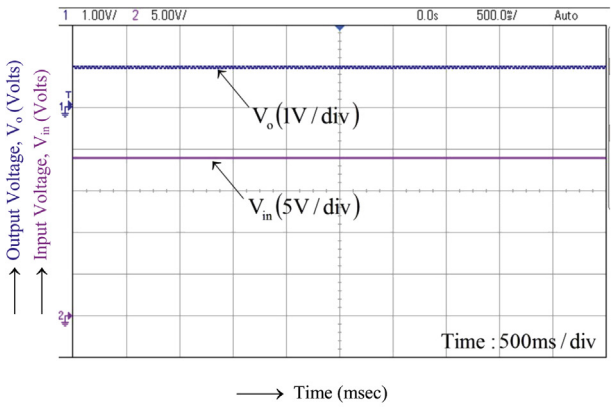

(b) Experimental results

Fig. 11 – Output voltage and input voltage waveforms. (a) Simulation results. (b) Experimental results.

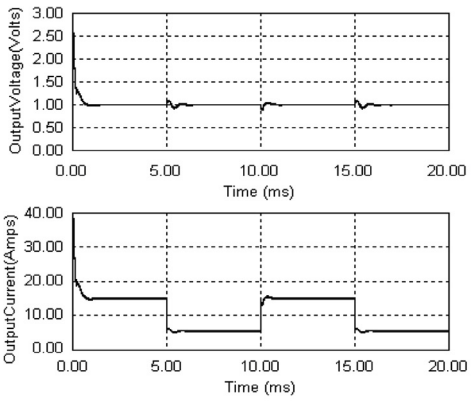

(a) Simulation results

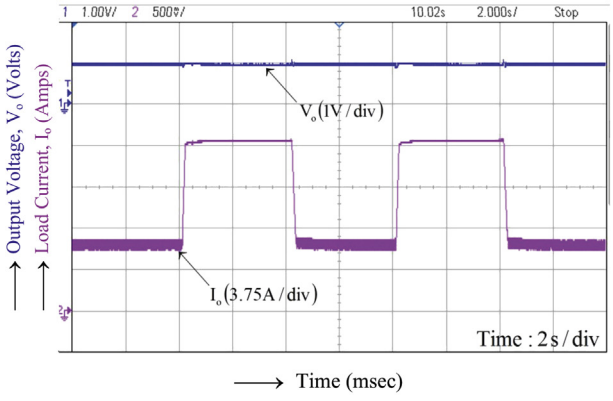

(b) Experimental results

Fig. 12 – Output voltage for periodic variation in load current. (a) Simulation results. (b) Experimental results.

Please cite this article as: RavindranathTagore Y et al., Modelling, simulation and control of a fuel cell-powered laptop computer voltage regulator module, International Journal of Hydrogen Energy, https://doi.org/10.1016/j.ijhydene.2019.02.141

Results and discussion

Controller performance for a stack voltage of 19 V at constant load current

When an input voltage of 19 V obtained from the ABFC stack is applied to the QBC with ACM controller, a constant output voltage of 1 V is maintained with negligible steady-state voltage ripple of ±1%, representing tight voltage regulation of the system. The simulation and experimental results shown in Fig. 11 (a) and Fig. 11 (b) are in close agreement.

Controller performance during periodic load variation from 5.6 A to 15 A and 15A-5.6 A for a stack input voltage of 19 V

For periodic load variation as shown in Fig. 12, the output voltage undergoes a transient voltage deviation of 10% rise during a step down load transient and a 10% fall during a step up load transient with a settling time of 0.85 msec, indicating fast dynamic response of the system. The simulation and experimental results are shown in Fig. 12 (a) and Fig. 12 (b). A good match is found between the simulation and experimental results.

The results show that the QBC provides tight output voltage regulation as well as good dynamic performance, which are stringent requirements for the CPU voltage regulator. The ABFC and QBC power system is a potential alternative for CPU power applications.

Conclusion

An ABFC and QBC power system was proposed for powering a laptop CPU core. Activation polarisation, ohmic polarisation and mass transfer effects were included in the model to simulate the actual behaviour of an ABFC. The model shows a good match with experimental results. The ABFC stack output voltage is unregulated and often not constant. The required dynamic performance is achieved with an ACM controller-based QBC in addition to tight voltage regulation. QBC hardware was developed and found to match closely with simulation results. From the results, it is evident that the proposed ABFC and QBC power system is well suited for CPU power applications. Hybrid power system like ABFC and lithium-ion battery combination can be investigated for further extending the life of the system as well as improving its efficiency.

REFERENCES

[1] Wang L, Husar A, Zhou T, LiuH. A parametric study of PEM fuel cell performances. Int J Hydrogen Energy 2003;28(11):1263–72. https://doi.org/10.1016/S0360-3199(02)00284-7.

[2] Yalcinoz T, Alam MS. Improved dynamic performance of hybrid PEM fuel cells and ultra capacitors for portable applications. Int J Hydrogen Energy 2008;33(7):1932–40. https://doi.org/10.1016/j.ijhydene.2008.01.027.

[3] Lopez Lopez Guadalupe, Rodriguez Ricardo Schacht, Alvarado Victor M, Gomez-Aguilar JF, Mota Juan E, Sandoval Cinda. Hybrid PEMFC-supercapacitor system: modeling and energy management in energetic macroscopic representation. J Applied Energy 2017;205:1478–94. https://doi.org/10.1016/j.apenergy.2017.08.063.

[4] Sandoval Cinda, Alvarado Victor M, Carmona Jean-Claude, Lopez Lopez Guadalupe, Gomez-Aguilar JF. Energy management control strategy to improve the FC/SC dynamic behavior on hybrid electric vehicles: a frequency based distribution. J Renewable Energy 2017;105:407–18. https://doi.org/10.1016/j.renene.2016.12.029.

[5] Rojas Alan Cruz, Lopez Lopez Guadalupe, Gomez-Aguilar JF, Alvarado Victor M, Sandoval Torres Cinda Luz. Control of the air supply subsystem in a PEMFC with balance of plant simulation. J Sustainability 2017;9(1):73. https://doi.org/10.3390/su9010073.

[6] Manoj Kumar P, Kolar Ajit Kumar. Effect of cathode channel dimensions on the performance of an air-breathing PEM fuel cell. Int J Thermal Sciences 2010;49(5):844–57. https://doi.org/10.1016/j.ijthermalsci.2009.12.002.

[7] Yadlapalli RT, Anuradha K. Comparative study of switched-mode power supplies for low voltage and high current applications. J Electr Eng 2016;16(1):316–29.

[8] Yadlapalli RT, Kotapati A. A fast-response sliding-mode controller for quadratic buck converter. Int J Power Electron 2014;6(2):103–30. https://doi.org/10.1504/IJPELEC.2014.061468.

[9] Kamiriski B, Wejrzanowski K, Koczara W. An application of PSIM simulation software for rapid prototyping of DSP based power electronics control systems. Proceedings of the IEEE 35th Annual Power Electronics Specialists Conference; 2004 June 20-25. Germany: Aachen; 2004. p. 336–41. https://doi.org/10.1109/PESC.2004.135576610.1109/TEC.2008.2011837.

[10] Amphlett JC, Baumertr M, Mannr F. Performance modeling of the Ballard mark IV solid polymer electrolyte fuel cell: empirical model development. J Electrochem Soc 1995;142(1):9–15. https://doi.org/10.1149/1.2043959.

[11] Kim J, Lees M, Srinivasan S. Modelling of proton exchange membrane fuel cell performance with an empirical equation. J Electrochem Soc 1995;142(8):2670–4. https://doi.org/10.1149/1.2050072.

[12] Sharifi Asl SM, Rowshanzamir S, Eikani MH. Modelling and simulation of the steady-state and dynamic behaviour of a PEM fuel cell. J Energy 2010 Apr;35(4):1633–46. https://doi.org/10.1016/j.energy.2009.12.010.

[13] Fuller TF, Newman J. Water and thermal management in solid polymer electrolyte fuel cells. J Electrochem Soc 1993;140(5):1218–25. https://doi.org/10.1149/1.2220960.

[14] Jia J, Li Q, Wang Y, Cham YT, Han M. Modeling and dynamic characteristic simulation of proton exchange membrane fuel cell. IEEE Trans Energy Convers 2008;24(1):283–91. https://doi.org/10.1109/TEC.2008.2011837.

Please cite this article as: RavindranathTagore Y et al., Modelling, simulation and control of a fuel cell-powered laptop computer voltage regulator module, International Journal of Hydrogen Energy, https://doi.org/10.1016/j.ijhydene.2019.02.141